

Fracture Surface Evaluation of Zircaloy - 4

VLADIMIR ALEXANDRU PAUN¹, VIOREL PUTU PAUN^{2*}

¹ Computer Science and Systems Engineering Department, ENSTA ParisTech, France

² Politehnica University of Bucharest, Physics Department, 202 Splaiul Independentei, 060022, Bucharest, Romania

One important direction for the mechanical behavior study of the materials is the fracture surface evaluation. This work makes a qualitative interpretation of the fracture surface from some Zircaloy-4 SEM microfractographies by using the fractal analysis technique. By reason of the current research, we introduce for the first time some new algorithms, most of them based on Box Counting methods and variations for 2D and 3D structures. The Box Counting algorithm is an efficient algorithm to compute the Fractal Dimension and can be applied directly on gray-levels images.

Keywords: fractal dimension, box-counting method, fracture surface, Zircaloy-4, images analysis

In mathematics dictionary, the word fractal defines a geometric pattern that is repeated at every scale and therefore it cannot be represented by a classical geometry, evidently. The fractal concept was first introduced by Mandelbrot [1], who used it as an indicator of surface roughness.

It was later applied by Pentland [2] in natural scene analysis and by Keller et al. [3] in textured image segmentation with the gray level replaced by the fractal dimension. The fractal dimension has been used in image classification to measure surface roughness where different natural scenes such as mountains, clouds, trees, and deserts generate different fractal dimensions. Of the wide variety of methods for estimating the fractal dimension that have so far been proposed [4], the box-counting method is one of the more widely used ones, as it can be computed automatically and can be applied to patterns with or without self-similarity.

Fractals, sets that exhibit certain self-similarity, have attracted considerable attention in the past decade [4, 5]. Considerable theoretical work has been done on fractals and related topics [6]. Application of fractals to various areas in engineering is fairly recent.

Zirconium is an attractive material in nuclear environment mainly because of its good neutron absorption properties. Its alloys, Zircaloy-2 and Zircaloy-4, are used for reactor components such as cladding, spacers and shroud or guide tubes. Today, Romanian power reactor fuels in production use Zircaloy-4, as per specifications of CANDU license.

To a complete understanding, CANDU (CANada Deuterium Uranium) reactor power plant uses heavy water (known as deuterium oxide, in chemical vocabulary) as a moderator, Zircaloy-4 tubes and natural, unenriched uranium (0.7% U-235) as a fuel. In respect of truth, Sandvik (a global company founded in 1862 in Sandviken, Sweden) manufactures Zircaloy-4 tubes to the CANDU nuclear fuel type. We mention also, that AECL, the manufacturer of CANDU reactors, has provided these reactors to governments/utilities in Argentina, India, Korea, Pakistan, and Romania. (See CANDU-technology, CANDU reactors, freely available on Internet.)

Of great interest are the thin walls Zircaloy-4 tubes, which are sometimes subjected to cyclic loadings that may initiate and propagate fatigue cracks. The cracks are usually initiated at flaws or stress concentrations. One

important direction for the mechanical behavior study of the materials is the fracture surface analysis. This work makes an evaluation of the fracture surface from some SEM microfractographies by using the fractal analysis technique.

Owing to the high degree of self-similarity exhibited by real data, fractals appear to be a promising tool for the fracture surface interpretation. A new algorithm for two-dimensional data analysis is proposed that is easy to implement and its computational complexity is low.

Experimental part

Theoretical Background and Algorithms

Generally expressed, a dynamical system consists of an abstract phase space or state space, whose coordinates describe the dynamical state at any instant. Consequently, a dynamical rule which specifies the immediate future trend of all state variables is necessary. Naturally, we take into account only the present values of those same state variables. In mathematical language, a dynamical system is described by an initial value problem.

In continuation, for a dynamical system to be chaotic it must have a *large* set of initial conditions which are highly unstable. No matter how precisely one measures the initial condition in these systems, the prediction of its subsequent motion goes radically wrong after a short time. Typically, the predictability horizon grows only logarithmically with the precision of measurement (for positive values of Lyapunov exponents).

Lyapunov exponents measure the rate at which nearby orbits converge or diverge. There are as many Lyapunov exponents as there are dimensions in the state space of the system, but the largest is usually the most important. Roughly speaking the (maximal) Lyapunov exponent is the time constant.

In his studies on complex geometrical shapes [7], Mandelbrot proposes the fractal theory in order to achieve a better characterization of different phenomena in physics, chemistry, biology and medicine.

The term *fractal dimension* is sometimes used to refer to what is more commonly called the *capacity dimension* (which is, roughly speaking, the exponent D in the expression $n(r) = r^{-D}$, where $n(r)$ is the minimum number of open sets of size r needed to cover the set). However, it can more generally refer to any of the dimensions commonly used to characterize fractals (e.g. capacity

*email: paun@physics.pub.ro

dimension, correlation dimension, information dimension, box counting dimension, Lyapunov dimension, Minkowski-Bouligand dimension).

In engineering practice, the fractal surfaces can be exhaustively characterized only by two parameters. In this sense, a non-integer Hausdorff-Besicovitch dimension D , named the fractal dimension and a scaling constant G , referred to as fractal roughness, are sufficient. The fractal dimension provides a quantitative description of how close a geometry is to being a point ($D=0$), a perfect line ($D=1$), a plane ($D=2$) or a volume ($D=3$). Being assessments of material surface, the dimensions of surface profiles are exclusively considered in the current work, and therefore $1 < D < 2$. In other papers G is sometimes called the fractal roughness parameter, as it may have influence on the height of a fractal rough surface. We will mention here that, undoubtedly, the fractal parameters can all be extracted from rough surface data.

Fractal dimensions

Hausdorff dimension D_H was introduced in 1918 by mathematician Felix Hausdorff. Since many of the technical developments used to compute the Hausdorff dimension for highly irregular sets were obtained by Abram Samoilovitch Besicovitch, D_H is sometimes called-Hausdorff-Besicovitch dimension. Hausdorff's original formulation is based on the construction of a particular measure, representing the uniform density of the fractal object. Intuitively, we can sum up the construction as follows: Let A be a fractal (object) and $C(r, A) = \{B_1, \dots, B_k\}$ a complete coverage of A consisting of spheres of diameter smaller than a given r that approximate A , so $\delta_i = \delta_i(B_i) < r$.

In this moment, we can define the Hausdorff measure as the function H_δ^D that identifies the smallest of all the covering spheres for A with $\delta < r$:

$$H_\delta^D(A) = \omega_D \lim_{r \rightarrow 0} \left\{ \inf \sum_i \delta_i^D \right\} \quad (1)$$

with ω_D volume of the unit sphere in R^D for integer D . Thereby, we obtain an approximate measurement of A , the so-called course-grained volume.

In continuation, a brief modern introduction for the Hausdorff dimension of a set embedded in the n -dimensional Euclidian space, is presented. Let

$$E^n = \{X | X = (x_1, \dots, x_n), x_i \in R\}, \quad (2)$$

for some natural number n . Then, define the diameter of some cover C as

$$diam(C) = \sup \{d_e(x, y) | x, y \in C\} \quad (3)$$

where:

$$d_e(x, y) = \sqrt{\sum_{i=1}^n (x_i - y_i)^2} \quad (4)$$

denotes the Euclidean distance function. Let $A \subset R^n$ and let C_1, C_2, \dots be an open cover of it. More precisely, an open cover of A is defined by covers C_i such that

$$A \subset \bigcup_{i=1}^{\infty} C_i \quad (5)$$

Then, for every positive numbers s and ε , let

$$h_\varepsilon^s(A) = \inf \left\{ \sum_i diam(C_i)^s \mid (C_i)_{\geq 0} \right. \\ \left. \text{is an open cover of } A, diam(C_i) \leq \varepsilon \right\} \quad (6)$$

so that the s -dimensional Hausdorff measure of A is

$$h^s(A) = \lim_{\varepsilon \rightarrow 0} h_\varepsilon^s(A). \quad (7)$$

It can be proved that there is a number $D_{HB}(A)$ such that $h^s(A) = \infty$ if $s < D_{HB}(A)$ and $h^s = 0$ if $s > D_{HB}(A)$. The number, the Hausdorff dimension of A , can be zero, infinite or a positive real number.

Then, the Hausdorff-Besicovitch (HB) fractal dimension of A is defined as

$$D_{HB}(A) = \inf \{s \mid h^s(A) = 0\} = \sup \{s \mid h^s(A) = \infty\} \quad (8)$$

Today, the general fractal dimension is most commonly defined as the particular Hausdorff-Besicovitch (HB) dimension.

Due to the complexity and impracticality of finding the optimal cover defined by the HB dimension, we need a different bounding estimate, i.e., one that is easily calculated.

One such upper bound estimation of the HB dimension is the box dimension definition.

Remark. Stricto sensu, fractal dimension allows us to measure the degree of complexity by evaluating how fast our measurements increase or decrease as our scale becomes larger or smaller. There are many different kinds of dimension. Further, no other theoretical developments, we can discuss here two types of fractal dimension: self-similarity dimension and box-counting dimension. A simple comparison shows that, the Box-counting dimension is much more widely used than the self-similarity dimension since the box-counting dimension can measure pictures that are not self-similar (and most real-life applications are not self-similar).

Other dimension types include topological dimension, Hausdorff dimension, and Euclidean dimension. It is important to note that not all types of dimension measurement will give the same answer to a single problem. However, our dimension measurements will give the same answer.

Box-counting method to estimate the fractal dimension

According to Matlab Tutorial, a possible characterization of a fractal set is provided by the *box-counting* method. More precisely, the number N of boxes of size R needed to cover a fractal set follows a power-law, $N = N_0 R^{-D_F}$, $D_F \leq D_s$. Here, D_s is the dimension of the space and $D_{sp} = 1, 2, 3$ respectively. D_F is known as the Minkowski-Bouligand dimension, or Kolmogorov capacity, or Kolmogorov dimension, or simply box-counting dimension. (Computing a fractal dimension with Matlab: 1D, 2D and 3D Box-counting)

In our box-counting method, an image measuring size $R \times R$ pixels is scaled down to $s \times s$, where $1 \leq s \leq R/2$ and s is an integer. Then $r = s/R$. The image is treated as a three-dimensional space, where two dimensions define the coordinates (x, y) of the pixels and the third coordinate (z) defines their grayscale values. The (x, y) is partitioned into grids measuring $s \times s$. On each grid there is a column of boxes measuring $s \times s \times s$. If the minimum and the maximum grayscale levels in the (i, j) th grid fall into, the k th and l th boxes, respectively, the contribution of n_r in the (i, j) th grid is defined as

$$n_r(i, j) = l - k + 1 \quad (9)$$

In this method $N(r)$ is defined as the summation of the contributions from all the grids that are located in a window of the image

$$N(r) = \sum_{i,j} n_r(i, j) \quad (10)$$

If $N(r) = N_r$ is computed for different values of r , then the fractal dimension can be estimated as the slope of the line that bestfits the points $(\log(1/r), \log N_r)$.

Finally, a straight line is fitted to the plotted points in the diagram using the least-squares method. In accordance with Mandelbrot's view, the linear regression equation used to estimate the fractal dimension is

$$\log(N_r) = \log(k) + D \log(1/r), \quad (11)$$

where k is a constant and D denotes the dimensions of the fractal set. For some mathematicians represents the lacunarity.

Box-counting algorithm

In recent time publications, the fractal and self-similarity properties of complex networks have attracted the scientists attention. In fact, especially after Song et al. found that a variety of real complex networks exhibit the self-similarity property. In particular mode, the box-covering algorithm is applied to calculate the fractal dimension of many real fractal-networks.

One of the most efficient methods to compute the Fractal Dimension is the Box-counting algorithm, [8, 9]. We will quickly, but conclusively, examine the classical Box Counting Method, which is widely used to determine the fractal dimension of objects with complicated shapes. In fact, the box counting method is analogous to the perimeter measuring method used in the past for the coastlines. However, in this case, we cover the image with a grid, and then count how many boxes of the grid are covering part of the image. Then we do the same thing but using a finer grid with smaller boxes. By shrinking the size of the grid repeatedly, we end up more accurately defining the structure of the analyzed pattern.

In another train of thoughts, the Box-counting algorithm is very appropriate particularly when the analysis is on two-dimensional datasets. The idea is to count the number of boxes in a minimal cover that contains at least one element of the set. This is then carried out for a sequence of decreasing box sizes.

Let us consider a picture (structure). We cover the structure with a number of square boxes of size s . We count the number of the boxes which contain some part of the structure and let $N(s)$ be this number. Clearly, if we increase the number of boxes or, equivalently, we decrease to p , we obtain $N(p)$. After this we make a diagram, on the Ox -axis we measure $-\log(s)$ and on Oy -axis we measure $\log(N(s))$. In this way we obtain several points for different values of s . The Box Counting Dimension of the structures is defined as the slope of the regression line defined by the points on the diagram. The Box Counting Dimension is a good approximation of the Hausdorff Dimension (Fractal Dimension). The usual Box Counting - type algorithms can be applied only to binary (black/white) images. In order to save the information, we developed an extended Box Counting - like algorithm version which can be apply directly on gray-levels images. The basic ideas associate to every pixel a weight proportional to its gray level. In this way we obtain a 3D-object on which we apply a 3D Box Counting algorithm and therefore we obtain an approximation of the Fractal Dimension (a number between 0 and 3). We call this number the Weighted Fractal Dimension (WFD), [8]. Let A be a pixel on an image and let K be a neighborhood of A . By using the 3D-Box Counting algorithm we compute the WFD of K . We repeat the process for every pixel in the image. In this way we obtain a matrix with inputs the WFD of every pixel respectively. We associate to every pixel a color according to its WFD (The association between the WFD and the color is conventional

and is a part of the algorithm). Finally, we generate a new image containing the level lines of the WFD's. We call this new image the Weighted Fractal Dimension Map (WFDMap), appellation that will be used everywhere in this study.

The application in Material Sciences and Applied Physics of the ideal fractals theory needs a good understanding of this concept, productively in the field of evaluating images.

Results and discussions

Creep rupture under constant loading

The fatigue mechanisms are known to researchers, largely, although some questions have not yet found the answer. However, how and why do fatigue cracks start in material structure? To understand the micromechanics of fatigue crack initiation, we need to know something about metals. Metals are crystalline in nature. Metal crystals are referred to as grains and are composed of uniform layers of atoms stacked one upon another like eggs in a crate [9].

The atoms occupy regular positions in what is called a lattice structure. The atomic forces keep the atoms in place, videlicet maintain the atoms instead of the default crystalline network. When a grain deforms these layers attempt to slide past each other in a shearing process called slip. If the slip displacement is small (confined to the elastic portion of the stress vs. strain curve) the deformation will be reversible. If the slip is large enough (exceeding the P.L.) plastic deformation will occur along the slip plane and the slip will be irreversible. Finally, after the accumulated fatigue in the structure of material tested, the fracture appears, relentlessly, as an irrevocable end.

At temperatures higher than $0.5 T_M$ (T_M = melting point), the time dependence of the strain and fracture characteristics of the materials becomes the central design problem for any device working under these conditions, [10].

Assuming constant loading, we decide that the creep influences the operation time of the material to be used, the strains which are taken into consideration are creep strains, and rupture is also creep rupture.

In principle, the trade alloys which are usually encountered have a creep fracture of intergranular type, and rupture occurs normally or by shearing.

At high stresses and low temperatures within the creeping domain, this rupture is due to the cavities in the triple points from the grains limit.

At small stresses and high temperatures the rupture can result from the generation and multiplication of the cavities along the grains limits, especially in the direction which is transversal to the applied stress. This process of cavities formation is known under the denomination of cavitations.

At some metals (e.g. high purity aluminum) no cavities have been noticed at the graining limit, and rupture occurs by pure shearing (in a rather ductile manner).

We can assert that certain conditions can favor an increasing tendency towards fragile like rupture.

A form of cracking at the under stress corrosion of copper can be considered as a result of the oxide film rupture.

In return, the oxygen absorbed from the atmosphere can facilitate cavities nucleation at the grains limit (cavitations); by excluding the oxygen from the testing conditions, the process of cavitations within copper decreases.

The micrographs used to illustrate the model developed above represent the Zircaloy-4 sheaths fracture, at a steady stress in time, by the so called dynamical burst test. Through this test we have attempted to simulate the accident conditions resulting from a loss of the cooling

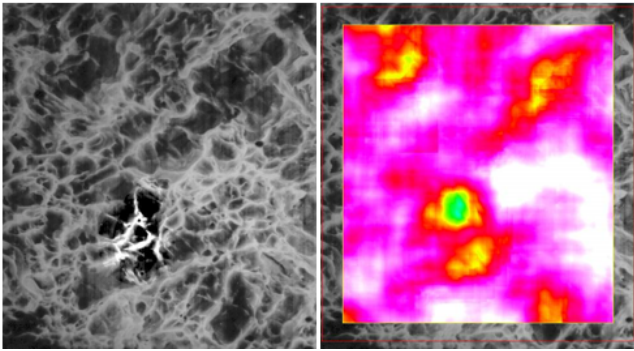


Fig.1.SEM micrographs from Zircaloy-4 specimens: first sample (x 1000)

that the average of the local fractal dimensions of the entire sample is 1.8983.

In figure 2, regarding the three highlighted zones (marked with yellow border), for three distinct areas of the image, the fractal dimensions are different. As seen in the right-hand side window, the fractal dimensions, corresponding to each surface delineated, are $D = 1.92$, $D=1.89$, respectively $D = 1.68$.

In figure 3 linear functions in log-log graphs (color lines) for direct extraction of fractal dimension and lacunarity, are presented (see sub-chapter 2.2).

In counterpart with WFDM filtration procedure, but conformable to the theory advanced in paragraph 2.2 of chapter 2, r is an array of box lengths, and N is the number

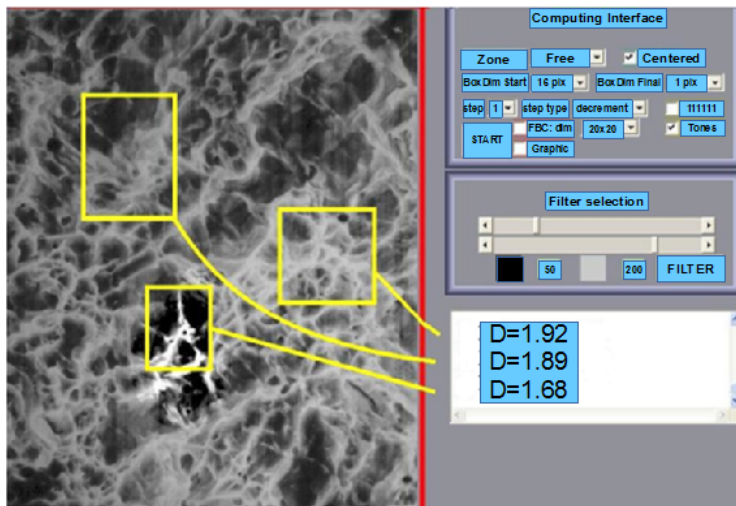


Fig.2. Local fractal dimensions of three different areas (first sample)

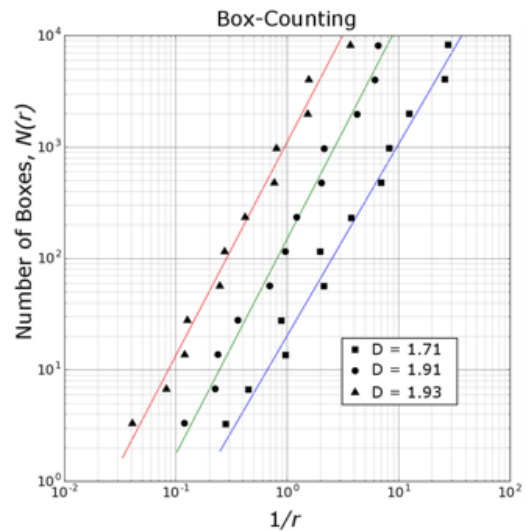


Fig. 3. $N(r)$ versus $1/r$ plotted on a log-log graphic

agent, LOCA (Loss Of Coolant Accident), and also to establish some failure criteria.

We have noticed the response of the studied material, namely the Zircaloy-4 sheath, under the given conditions, and in a biaxial stress state. The rupture was a specific one of intergranular type, which was to be expected, Zircaloy-4 being a ductile material during creep occurring in a dynamical burst test.

Remark. The same material Zircaloy-4, verified in other consecrate tests [11, 12], responded perfectly comparable, which proves the fractal nature of rupture for metal and metal alloys, truth certified by Mandelbrot [13] and questioned (however) on various other materials of a not different category [14].

Applications

In this section we apply the previous algorithm and the WFDM method to detect deficiencies in several samples of Zircaloy-4 [10]. We look for modifications in the WFDM associated to the areas with deficiencies. The study was done on 20 microfractographies and in all these cases the regions with deficiencies were revealed by the WFDM. The reason is that there are significant differences of the fractal dimensions between the normal areas and the modified areas. We present below 3 of these samples.

On the left we have a sample of Zircaloy-4, and on the right we have the associated WFDM of it. On the map one can see a small area with a different color from the background (green). The reason is shown below where we present the result of computation of the local fractal dimensions of three different areas, including the deficiency (green colored on the WFDM). One can observe significant differences between the local fractal dimensions between the two normal areas and the modified one. We mention

of boxes needed to cover the fractal for a given box length on picture. Counted values were represented in figure 3, respectively N against $1/r$ was plotted on a log-log graphic, so that we will have a positive linear relationship. Before plotting anything onto the map, the data has been modeled using adequate software. In conclusion, the fractal dimensions, corresponding to the slopes of each color line, are: $D = 1.93$, $D = 1.91$ and $D = 1.71$.

In the next pictures we present the result of WFDM filtration in order to point out the deficiency. On the left we have the histogram of the fractal dimensions.

As seen immediately (figs. 4, 6 and 8) the images representing WFDM filtration stage look different one with respect to another (fig. 4b), fig. 6 b) and fig. 8 b)), which translates into a difference of shape and surface for three representations of fractal dimensions histograms (fig. 4 a), fig. 6 a) and fig. 8)).

Fractal dimension is an important quantitative characteristic of a picture in fractal analysis of fracture SEM images. In this evaluation technique, the box-counting

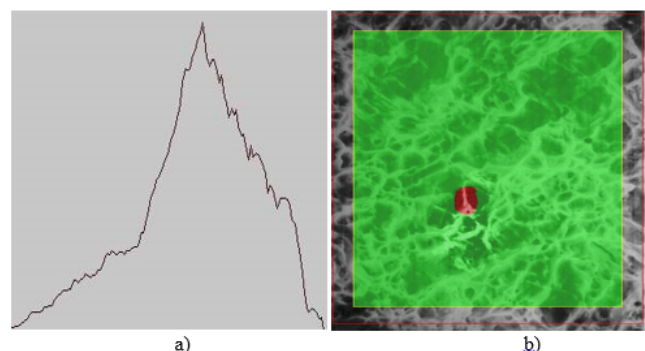


Fig. 4. a) Fractal dimensions histogram; b) WFDM filtration

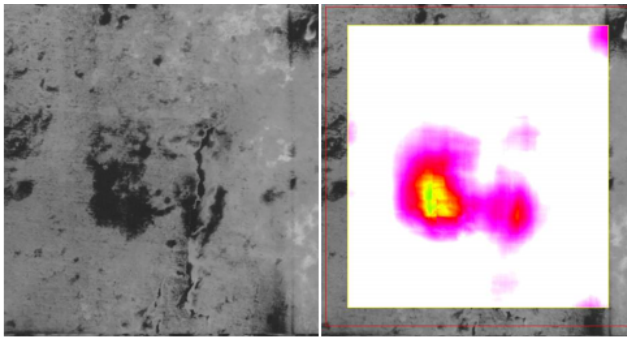


Fig. 5. SEM micrographs from Zircaloy-4 specimens: the second sample (x100)

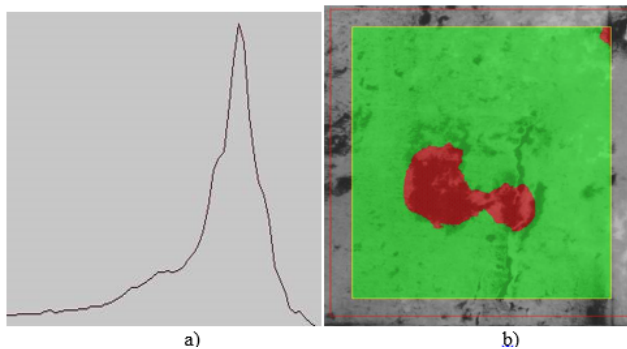


Fig. 6. a) Fractal dimensions histogram; b) WFDM filtration

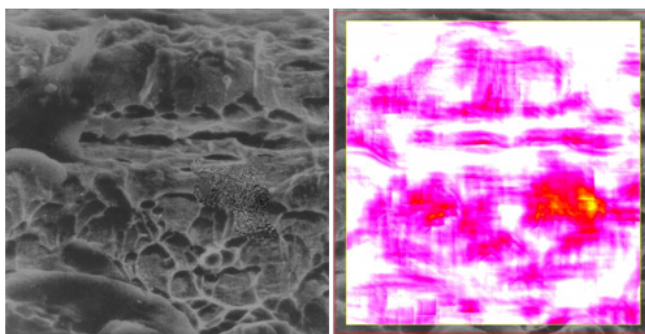


Fig. 7. SEM micrographs from Zircaloy-4 specimens: the third sample(x1000)

method is one of many calculation methods of a fractal dimension, without question. Due to its simple calculation, it has been frequently used in engineering and medical successful investigation.

In terms of phenomenological interpretation, the SEM microfractographies studied correspond to the response of the material in a biaxial stress state. The rupture was a specific one of intergranular type, as being expected, Zircaloy-4 being a ductile material during the creep occurring in a dynamical burst test. It most likely occurred as a result of cavities nucleation in the triple points at the grains limit, due to the increase of these cavities and their coalescence, process which is called cavitations, best illustrated by figure 7.

The cavities which have been put in evidence are wedge shaped cavities (type *W* cavities). In brief, they arise at the junctions of the grain limit, as a result of its slipping, due to a massive strain concentration in a triple point. When the radius of the cavity becomes large enough, a micro fissure occurs. These micro fissures are obvious when approaching the rupture area.

Putting together the old mathematical problem of fractal dimension as well as this new approach, the present study follows and continues the vision in the papers written by Song et al [15, 16], the first one published in Nature 2005 [15], and respectively Schneider et al [17].

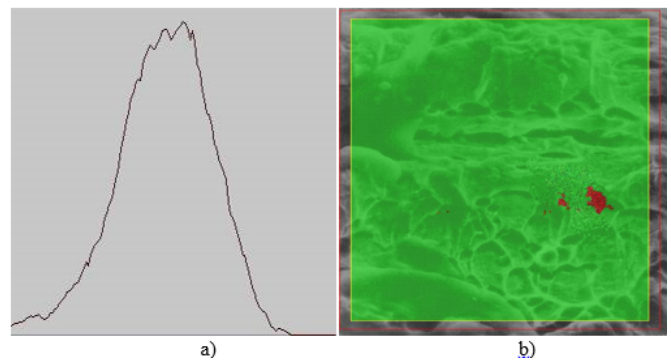


Fig. 8. a) Fractal dimensions histogram; b) WFDM filtration

Last but not least, reading the Mandelbrot book [18], much later than it was written, it made possible the connection between our experimental data and their new reinterpretation by the logic of fractal analysis.

By virtue of obtaining a better resolution of digitized SEM images, it is advised into a few articles in the field [19, 20], that a realistic area estimation from grayscale images could go up to the nanosurface level, as the last one shows [20].

In the future contributions of some new research work, we intend to corroborate the method of fractal analysis with time series method, the last method widely presented in a paper published by the second author [21].

Conclusions

This paper presents a qualitative analysis of Zircaloy-4 fracture experimental data.

By re-examining the box dimension definition, a mathematical dual problem for its estimation, based on the box counting algorithm was presented. This dual problem assumes the number of covering elements is known and one only needs to find the optimal placement and size of the covering elements.

A new algorithm based on correlation dimension for two-dimensional data is proposed.

The Box Counting algorithm is simple to implement and has low computational complexity. Experiments applying the algorithm to different micrographs are presented and confirm the suitability of the approach for this application.

The WFDM method is a powerful tool for the detection of most deficiencies of the Zircaloy-4 material. As expected, the fractal dimension changes with the matrix used.

Finally, we demonstrate that obtaining fractal structures in the Zircaloy-4 SEM fractographies is a realistic presumption and the fractal descriptions of the fracture parameters are a good micro structural analysis.

References

1. MANDELBROT, B. B., Les objets fractals, forme, hasard et dimension, Flammarion, Paris, 1975
2. PENTLAND, A., IEEE Trans. Pattern Anal. Mach. Intell., **6**, 1984, p. 666
3. KELLER, J.M., CHEN, S., CROWNOVER, R.M., **45**, 1989, p. 150
4. PEITGEN, H.-O., JURGENS, H., SAUPE, D., Chaos and Fractals. New Frontiers of Science, Springer, 1992
5. FALCONER, K., Fractal Geometry – Mathematical Foundations and Application, John Wiley and Sons, New York, 1990
6. STEEB, W.-H., The Nonlinear Workbook: Chaos, Fractals, Cellular Automata, Genetic Algorithms, Gene Expression Programming, Support Vector Machine, Wavelets, Hidden ... Java and Symbolic C++ Programs, World Scientific Publishing Company, 6th Revised edition, 2014
7. MANDELBROT, B.B., The Fractal Geometry of Nature, W. H. Freeman and Company, New York, 1982
8. OLTEANU, M., PAUN, V.P., TANASE, M., Rev. Chim. (Bucharest), **56**, no.1, 2005, p. 97

9. OLTEANU, M., PAUN, V.P., TANASE, M., Rev. Chim. (Bucharest), **56**, no.7, 2005
10. PAUN, V.-P., Mat. Plast., **41**, no.4, 2004, p. 262
11. PAUN, V. P., CIUCU, C., Rev. Chim. (Bucharest), **54**, no.12, 2003, p. 957
12. PAUN, V. P., Mat. Plast., **40**, no. 3, 2003, p.127
13. MANDELBROT, B. B., D.E. PASSOJA, D. E., PAULLAY, A.J., Nature, **308**, 1984, p. 771
14. IORDACHE, D., PUSCA, S., TOMA, G., PAUN, V.P., STERIAN, A., MORARESCU, C., Lect Notes Comput SC, **3980**, 2006, p.804
15. SONG, C., HAVLIN, S., MAKSE, H.A., Nature, **433**, 2005, p. 392
16. SONG, C., GALLOS, L. K., HAVLIN, S., MAKSE, H.A., J. Stat. Mech: Theory Exp.2007, P03006, 2007
17. SCHNEIDER, C. M., KESSELRING, T. A., ANDRADE JR, J. S., HERRMANN, H.J., Phys. Rev. E, **86**, 016707, 2012
18. FRAME, M., MANDELBROT, B. B., NEGER, N., Fractal Geometry, Yale University, 2009
19. RUSS, J. C., Journal of Computer Assisted Microscopy, **3**, nr. 3, 1991, p. 127
20. BORSOS, Z., DINU, O., PAUN, V. P., U.P.B. Sci. Bull., Series A, **76**, nr.4, 2014, p.199
21. PAUN, V. P., Central European Journal of Physics, **7**, nr. 2, 2009, p. 264

Manuscript received: 15.01.2016